PCCP

Accepted Manuscript

This is an *Accepted Manuscript*, which has been through the Royal Society of Chemistry peer review process and has been accepted for publication.

Accepted Manuscripts are published online shortly after acceptance, before technical editing, formatting and proof reading. Using this free service, authors can make their results available to the community, in citable form, before we publish the edited article. We will replace this *Accepted Manuscript* with the edited and formatted *Advance Article* as soon as it is available.

You can find more information about *Accepted Manuscripts* in the Information for Authors.

Please note that technical editing may introduce minor changes to the text and/or graphics, which may alter content. The journal's standard Terms & Conditions and the Ethical guidelines still apply. In no event shall the Royal Society of Chemistry be held responsible for any errors or omissions in this *Accepted Manuscript* or any consequences arising from the use of any information it contains.

ROYAL SOCIETY OF CHEMISTRY

www.rsc.org/pccp

Theoretical Studies on the Quinoidal Thiophene Based Dyes for Dye Sensitized Solar Cell and NLO applications

R. Nithya and K. Senthilkumar

Department of Physics, Bharathiar University, Coimbatore, India-641 046.

*Corresponding author: Fax No: +91-422-2422387, E-Mail: ksenthil@buc.edu.in

Abstract

A series of quinoidal thiophene based dye molecules were designed and their optoelectronic properties were studied for dye sensitized solar cell (DSSC) applications. The efficiency of the designed dye molecules was analyzed using various parameters such as HOMO-LUMO energy gap, absorption spectra, light harvesting efficiency (LHE), exciton biding energy (E_b) and free energy change for electron injection (ΔG_{inject}). The simulated absorption spectra of the quinoidal thiophene molecules show that the electron withdrawing group substituted molecules exhibit dual band characteristics. We found that the cyano-[5'-(4''-amino benzylidene)-5H-thiophen-2'-ylidene] acetic acid based molecules, QT2B, QT4B, QT5 and QT6 are good candidates for DSSC application. Further, the study on the polarizability and hyperpolarizability of the designed molecules show that the electron withdrawing group substituted QT2B-X molecules (X=Cl, Br, CF_3, CN and NO_2) are good candidates for NLO application.

Keywords : DSSC, quinoidal thiophene dyes, absorption spectra, DFT and NLO property

Physical Chemistry Chemical Physics Accepted Manuscript

1. Introduction

The current interest of many researchers worldwide is to find an alternate renewable energy source to meet the energy crisis that is raised in this century. In this scenario, the utilization of sun light to produce electricity through the dye sensitized solar cell (DSSC) has become the key solution to meet the energy demand.[1-5] The dye molecule in DSSC is responsible for harvesting the solar light and injection of electrons into the conduction band of the semiconductor. The Ruthenium (Ru) complex such as N3, N719 and black dye are the most promising dye sensitizers with the photoelectric conversion efficiency of about 11%.[6-9] Recently, it has been reported that porphyrin sensitizer, SM315 exhibits a power conversion efficiency of about 13%, and it has been shown in an earlier study that the porphyrin sensitizer has a photoelectric conversion efficiency greater than 10%[10, 11]. However, the DSSC's based on the above dyes are expensive, difficult to purify and are hazardous to environment. Hence, the metal free organic dyes have been studied as an alternative to inorganic dyes for solar cell application. The advantages of organic sensitizers are low-cost production, easy availability, environmental friendly and flexible to structural modification. One typical way of designing an organic sensitizer is of the type D-π-A i.e. a donor group and an acceptor group is linked through the π-spacer.[3] The organic sensitizer of this type allows flexible structural modification through the substitution of different donor, acceptor and π-spacer. This strategy helps to tune the highest occupied molecular orbital (HOMO) and lowest unoccupied molecular orbital (LUMO) and extend the absorption spectra of the dye molecule. Several organic molecules such as coumarin, indoline, squaraine, anthracene, merocyanine, carbozole, pyrene and etc., were used as sensitizers and an extensive studies were performed both experimentally and theoretically to improve the efficiency of the DSSC.[3, 12-18] The theoretical studies on the dye sensitizer provide

Physical Chemistry Chemical Physics Accepted Manuscript

an insight into the photophysical property, orbital energies and to rationalize molecules with new functional groups.

Although, a number of organic molecules were studied for DSSC application, there is an urge to design new DSSC with improved electronic properties. Recently, Komatsu et al.[19] have synthesized quninoidal thiophene based DSSC and recorded a photoelectric conversion efficiency of about 5.2%. The simple strategy to improve the efficiency of DSSC is by increasing the π-conjugation of the molecule and the substitution of proper donor and acceptor groups.[3, 20] The chemical structure of the designed cyano-[5'-(4''-amino benzylidene)-5H-thiophen-2'-ylidene] acetic acid based new molecules are shown in Figure 1. The dye molecules, QT1-QT6 were constructed with the usual donor - π-spacer - acceptor strategy (D-π-A). Thiophene is an important π-conjugated organic molecule used for the applications in molecular electronics and solar cell fabrication, due to its high structural stability and π-conjugation.[21-23] It has been reported that the thiophene ring in quninoid form provides a more effective π-conjugation[19] and the sensitizer with minimum number of π-spacer was able to produce an intense absorption spectra with moderate efficiency. In the present study, one or two thiophene rings in quninoid form is used as the π-spacer and the different donor groups such as dimethyl-phenylamine, triphenylamine and methoxy substituted triphenylamine groups were substituted to increase the π-conjugation of the molecule and the acceptor group is the cynoacrylic acid. Previous theoretical studis[24, 25]on the DSSC have reported that the substitution of suitable donor group will enhance the performance of the cell, hence, in the present work, dye molecules with different donor groups were also studied.

In the present study, the opto-electronic properties of the designed molecules were studied using density functional theory (DFT) methods. In addition to this, the effect of

Physical Chemistry Chemical Physics Accepted Manuscript

substitution of electron withdrawing groups such as Cl, Br, CF_3, CN and NO_2 at the thiophene ring on the spectral properties and on the efficiency of the dye molecules have been studied. The efficiency of the designed quinoidal thiophene dye molecules was studied through the HOMO and LUMO energy levels, absorption spectra, light harvesting efficiency (LHE), exciton binding energy (E_b) and the free energy change for electron injection. It has been reported in the previous studies,[26-28] that the organic molecules with donor - π-spacer - acceptor combination exhibit good nonlinear optical (NLO) property. Further, it is reported that the NLO property of the molecule is sensitive to conjugation length, donor and acceptor substitutions and to the symmetry of the molecule.[26-29] The strategy followed here to design DSSC provides asymmetry in the molecule thereby favouring the NLO property. Hence, in the present work the NLO property of the designed quinoidal thiophene molecules was analyzed through the dipole moment, static polarizability and first hyperpolarizability.

2. Computational Methodology

The ground state geometries of the dye molecules were optimized at B3LYP[30-32] method with 6-311G(d,p) basis set. Consequently, the frequency calculation at the same level of theory show that the designed quinoidal thiophene dyes are at stationary points without any imaginary frequency. To include the solvent effect, the self consistent reaction field (SCRF) calculation has been performed using Tomasi's[33] polarizable continuum model (PCM). In PCM method, the solute molecule is lying inside a cavity representing a solvent medium defined in terms of structure less material characterized by its dielectric constant, radius, density and molecular volume. In the present study, the dielectric constant of 35.69 is used to represent the acetonitrile medium. The experimental absorption wavelength of QT1 molecule in acetonitrile medium is observed at 548 nm.[19] Based on the ground state optimized geometry, the absorption spectra of

Physical Chemistry Chemical Physics Accepted Manuscript

the QT1 molecule was calculated using the different DFT functionals within the framework of time dependent DFT (TDDFT) method. Manzhos et al.[34] have reported that TDDFT method fails to predict excitation energy of organic dyes. However, few benchmark studies[35, 36] on organic dyes have reported that the results obtained from TDDFT method is comparable with the highly accurate ab initio methods. In the present work, the absorption energy and oscillator strength associated with $\mathrm{HOMO} \rightarrow \mathrm{LUMO}$ transition in QT1 molecule calculated using B3LYP, PBE0,[37, 38] BHandHLYP,[31, 39] M06-2X,[40] M06-HF,[41] CAM-B3LYP[42] and LC-BLYP[43, 44] functionals with the 6-311G(d,p) basis set are summarized in Table S1a. Among the different functionals employed, the difference between the experimental and calculated absorption wavelength of QT1 molecule at B3LYP method is less and is found to be 19 nm. Further, the basis set effect on the absorption spectra of QT1 molecule was studied and their results are summarized in Table S1b. From Table S1b, it has been observed that the B3LYP functional with the 6-311+G(2d,2p) basis set predict the absorption spectra more closer to the experimental value. Hence, the absorption spectra of the designed quinoidal thiophene molecules in acetonitrile medium was calculated at B3LYP/6-311+G(2d,2p) level of theory. The B3LYP hybrid functional is one of the standard functionals and widely used to study the opto-electronic properties of the dye molecules.[45-47] The SWizard program[48, 49] has been used to simulate the absorption spectra of the molecules. The spectra were generated using the Gaussian function with half-bandwidth of 3000 cm^{-1} as given in the following relation,

$$\varepsilon(\omega) = c^2 \sum_I \frac{f_I}{\Delta_{1/2,I}} \exp\left(-2.773 \frac{(\omega - \omega_I)^2}{\Delta^2_{I/2,I}} \right)$$

where, $\varepsilon(\omega)$ is the molar extinction coefficient in M^{-1} cm^{-1}, ω is the energy of the allowed transition in cm^{-1}, f_I is the oscillator strength and $\Delta_{1/2}$ is the half-bandwidth.

Physical Chemistry Chemical Physics Accepted Manuscript

3. Results and Discussion

3.1 Frontier Molecular Orbitals

An extensive knowledge about the frontier molecular orbitals of organic molecules is important while studying the opto-electronic properties of the molecules. The highest occupied molecular orbital (HOMO), lowest unoccupied molecular orbital (LUMO) energies and energy gap between them of the quinoidal thiophene dyes calculated at B3LYP/6-311+G(2d,2p) level of theory in acetonitrile medium is illustrated in Figure 2. An efficient sensitizer should have a small HOMO-LUMO (E_{H-L}) gap, LUMO energy level above the conduction band of the semiconductor and HOMO energy level below the redox couple. From Figure 2, it is observed that except for QT2B-CF_3, CN and NO_2 substituted molecules, the LUMO energy of the dye molecules are above the conduction band of TiO_2 (-4.0 eV)[50] and the HOMO energies are below the redox couple of I^-/I_3^- (-4.8 eV).[51] The E_{H-L} of the QT1 dye molecule is 2.41 eV and the E_{H-L} of the other substituted dye molecules has decreased significantly. When the π-conjugation of QT1 molecule is increased with the substitution of another thiophene ring the E_{H-L} decreased by 0.5 eV from that of QT1. It is interesting to note that when the thiophene rings are in opposite direction (QT2B) the E_{H-L} has further decreased by 0.06 eV with respect to QT2A molecule. When the dimethyl-phenylamine group was replaced by triphenylamine group (QT3) in the donor part, the E_{H-L} of the dye molecule has decreased only by 0.08 eV with respect to QT1. Further, the QT4A and QT4B molecules were designed by extending the π-bridge of QT3 molecule with the substitution of another thiophene ring. The inclusion of second thiophene ring decreases the E_{H-L} by 0.43 and 0.49 eV with respect to QT3 in QT4A and QT4B dye molecules. In QT5 the methoxy group was substituted at the para position of the phenyl rings and in QT6 one of the phenyl rings was replaced with naphthyl ring. As shown in Figure 2, the methoxy

Physical Chemistry Chemical Physics Accepted Manuscript

group has slightly higher influence on the orbital energies than the naphthyl ring and the calculated E_{H-L} of QT5 molecule is 1.78 eV. By comparing the E_{H-L} of QT2B, QT4B, QT5 and QT6, it has been found that the E_{H-L} of the dye molecules does not show significant difference with the substitution of dimethyl-phenylamine, triphenylamine and the naphthalene group as donor group in the dye molecule. The substitution of strong electron withdrawing groups Cl, Br, CF_3, CN or NO_2 at the 3rd and 4th positions of the thiophene ring of QT2B molecule altered the HOMO and LUMO energies significantly. The CF_3 substituted molecule exhibit the minimum E_{H-L} of 1.53 eV. The E_{H-L} of the designed molecules ranges between 1.53 - 2.41 eV, indicating the effect of π-conjugation and substitution of functional groups on the energy levels of the dye molecules. From Figures 2-4, it has been observed that the substitution of strong electron withdrawing group has significant effect on the HOMO and LUMO energy levels of designed dye molecules than that of the extension of the π-conjugation through quinoid thiophene molecules.

The ground state density plot of the HOMO and LUMO of quinoidal thiophene molecules calculated at B3LYP/6-311G(d,p) level of theory in acetonitrile medium is shown in Figures 3 and 4, respectively. From Figure 3, it has been observed that the HOMO of QT1-QT6 is delocalized over the entire molecule and the LUMO of QT1, QT2A and QT2B is delocalized over the entire molecule, whereas the LUMO of QT3, QT4, QT5 and QT6 is delocalized on the π-bridge and on the acceptor group. Notably, the HOMO and LUMO delocalization on EWG substituted molecules, QT2B-X (X= Cl, Br, CF_3, CN and NO_2) is distinct from that of the other molecules. The HOMO of Cl and Br substituted molecules, (i.e QT2B-Cl and QT2B-Br) is delocalized over the entire molecule but with strong delocalization on one of the thiophene ring and on the acceptor group, and their LUMO is delocalized over the entire molecule. In the case

Physical Chemistry Chemical Physics Accepted Manuscript

of CF_3, CN and NO_2 substituted molecules, the HOMO is delocalized on one of the thiophene rings and on the acceptor group, whereas the LUMO is delocalized on the donor group and on the nearby thiophene ring. This distinct feature of the molecules is due to the substitution of strong EWGs on the thiophene rings. But for a molecule to have high electron injection and improved efficiency, the LUMO should be delocalized on the acceptor group. This shows that the EWG CF_3, CN and NO_2 substituted molecules cannot be used for the DSSC application. These results clearly show that the absorption spectra of the designed dye molecule is associated with the intramolecular charge transfer and $\pi \rightarrow \pi^*$ transition in the studied dye molecules.

3.2 Absorption Spectra

The absorption spectra of the quinoidal thiophene molecules calculated at TD-B3LYP/6-311+G(2d,2p) level of theory in acetonitrile medium is summarized in Table 1 and the simulated absorption spectra using SWizard program are shown in Figure 5. From Table 1 and Figure 5, it has been observed that the absorption spectra of the designed molecules have significantly red shifted with respect to the QT1 dye molecule. When the π-bridge of the QT1 molecule is increased by substituting another thiophene ring, the absorption spectra of the dye molecule is red shifted by 122 nm. The dominant absorption band of QT2A is observed at 661 nm, and if the two thiophene rings are in opposite direction (QT2B) the absorption spectra has been further red shifted by about 20 nm. The above results clearly show that the extension of π-conjugation through the quinoidal thiophene ring provides an effective conjugation and red shifts the absorption spectra significantly. In all the studied molecules, the dominant band is associated with HOMO $\rightarrow$ LUMO transition. When the donor group dimethyl-phenylamine was replaced by triphenylamine group (QT3) there was a red shift of 45 nm in the absorption spectra with respect to the QT1 molecule. The dominant absorption spectra of the QT3 dye molecule is found at 584

Physical Chemistry Chemical Physics Accepted Manuscript

nm and it corresponds to HOMO→LUMO transition and the small peaks observed at 408 and 327 nm are due to the electronic transition between HOMO-1→LUMO and HOMO-4→LUMO orbitals. The dominant absorption spectra of QT4A and QT4B molecules were observed at 693 and 713 nm. While comparing QT5 and QT6 molecules, the former exhibit the maximum absorption wavelength of 739 nm. As shown in Figure 5, the dominant absorption spectra of the QT1-QT6 dye molecules lie in the visible region of the spectrum.

From Figure 5, it has been observed that with substitution of EWG, the absorption spectra of the dye molecules exhibit dual band character i.e., one band lie in the visible region and the other band in the near IR region of the spectrum. This is in agreement with previous study[52] which has reported that the substitution of functional groups such as Se and Te, on the π-bridge provides dual band character. Among the EWG substituted molecules, the CF_3 substituted dye molecule (QT2B-CF_3) exhibit the maximum absorption wavelength at 1043 nm and it corresponds to HOMO→LUMO transition. But the intensity of the spectrum observed in the near IR region is weak, whereas the other band of QT2B-CF_3 observed at 451 nm is intense and it corresponds to HOMO-1→LUMO transition. In line with the previous study,[52] it has been observed that the absorption spectrum of the dye molecules have red shifted significantly, due to the substitution of strong EWG on the QT2B molecule. The density plot of the orbitals involved in electronic transitions is shown in Figures 3, 4 and S1. The molecular orbital analysis show that the dominant absorption bands of the dye molecule is either due to intramolecular charge transfer (ICT) or π→π* transition. The above results show that increase in the π-conjugation and the substitution of EWGs on the π-spacer, significantly red shift the absorption spectra of the designed molecules.

Physical Chemistry Chemical Physics Accepted Manuscript

The oscillator strength of the dye molecules has increased with the increase in the π-conjugation. From Table 1, it has been observed that the oscillator strength corresponding to dominant absorption band of QT2A (1.95) and QT2B (1.86) molecules have increased when compared with QT1 (1.38), showing that the substitution of quinoidal ring has enhanced the intensity of the absorption spectrum. Similar to QT2 molecules, the oscillator strength of QT4, QT5 and QT6 molecules is also high. As discussed previously, the EWG substituted molecules exhibit dual band character but their oscillator strength is lesser than that of the other molecules. It has been observed that the oscillator strength of the NO_2 substituted molecule is much lesser than the other molecules. The light harvesting efficiency (LHE) is one of the important parameter related with the intensity of the absorption spectra of the dye molecule and is calculated using the following equation

$$LHE = 1 - 10^{-f} \quad (1)$$

where, f is the oscillator strength of the dye molecule. For an efficient photocurrent response, the LHE of the dye molecule should be high. The calculated LHE for various bands of the designed dye molecules is summarized in Table 1. The LHE of the designed dye molecules has increased with the increase in the π-conjugation and is nearer to unity for the absorption band associated with HOMO $\rightarrow$ LUMO transition in the designed molecules except for QT2B-X (X=Br, CF_3, CN or NO_2) molecules. The maximum value of around 0.988 is observed for QT2A, QT2B, QT4A, QT4B, QT5 and QT6 molecules. Notably, for QT2B-CF_3 molecule the LHE of second absorption band appeared at 451 nm is 0.928, whereas for other EWG substituted dyes, the LHE is relatively lesser than that of QT1-QT6 molecules.

Physical Chemistry Chemical Physics Accepted Manuscript

3.3 Electron Injection and Exciton Binding Energy

The knowledge on the electronic properties of the dye molecules in the excited state is important to improve the performance of the DSSC. The efficiency of the solar cell is highly dependent on the rate of electron injection from the excited state of the dye molecule to the conduction band of the semiconductor. Preat et al.[53-55] theoretically proposed a method to quantify the electron injection from the excited state of the dye molecule to the conduction band of the semiconductor. According to this model, the free energy change (in eV) for the electron injection is expressed as

$$\Delta G_{inject} = E_{OX}^{dye^*} - E_{CB}^{SC} \qquad (2)$$

where, $E_{OX}^{dye^*}$ is the oxidation potential of the dye in the excited state and E_{CB}^{SC} is the conduction band edge of the semiconductor. E_{CB}^{SC} is sensitive to the experimental condition, for TiO_2 it is equal to 4.0 eV, which is the experimental value corresponding to the condition where the semiconductor (TiO_2) is in contact with the aqueous redox electrolyte of fixed pH 7.0.[50, 56] In general, two methods are commonly used to evaluate $E_{OX}^{dye^*}$. In the first method, it is assumed that the electron injection occurs from the unrelaxed excited state of the dye molecule, and the excited state oxidation potential is calculated from the redox potential of the ground state (E_{OX}^{dye}) (i.e., $-E_{HOMO}^{dye} = E_{OX}^{dye}$) and the absorption energy associated with the photoinduced intramolecular charge transfer ($\lambda_{\max}$)

$$E_{OX}^{dye^*} = E_{OX}^{dye} - \lambda_{\max} \qquad (3)$$

In the second method, it is assumed that the electron injection occurs from the relaxed excited state of the dye molecule and $E_{OX}^{dye^*}$ is calculated as

Physical Chemistry Chemical Physics Accepted Manuscript

$$E_{OX}^{dye^*} = E_{OX}^{dye} - E_{0-0}^{dye} \quad (4)$$

The 0-0 transition energy (E_{0-0}^{dye}) is calculated using λ_{max}, total energy of first excited state in ground state geometry $E_{S1}(Q_{S0})$ and the total energy of first excited state in excited state geometry $E_{S1}(Q_{S1})$ as

$$E_{0-0}^{dye} = \lambda_{max} - E_{S1}(Q_{S0}) - E_{S1}(Q_{S1}) \quad (5)$$

The excited state geometry of the dye molecules is optimized at TD-B3LYP/6-311G(d,p) level of theory in acetonitrile medium. The calculated $E_{OX}^{dye^*}$ and ΔG_{inject} through two methods are summarized in Table 2. For the effective functioning of the solar cell, the rate of electron injection from the dye molecule to the conduction band of the semiconductor should be high. From Table 2, it has been observed that QT1 molecule has high ΔG_{inject} of -0.80 eV and -0.75 eV calculated through the unrelaxed and relaxed models, respectively. By comparing the ΔG_{inject} calculated with the relaxed and unrelaxed geometries, it is found that for the QT3 and EWGs substituted Q2TB-X molecules the difference between ΔG_{inject} values calculated from two methods ranges between 0.1 to 0.35 eV, whereas for other molecules the difference is around 0.05 to 0.08 eV only. That is, the effect of relaxation on ΔG_{inject} of QT3 and Q2TB-X molecules is high and the ΔG_{inject} increases due to structural relaxation which is less favorable for photo current conversion efficiency. Except for EWGs substituted QT2B-X (X=Cl, Br, CF_3, CN and NO_2) molecules, the calculated ΔG_{inject} is negative implying that they are exergonic injection reaction which is favourable for electron transfer.[57] Notably, the EWG substituted dye molecules have high ΔG_{inject} and particularly the CF_3, CN and NO_2 substituted molecules have endoergic electron injection characteristics.

Physical Chemistry Chemical Physics Accepted Manuscript

To attain high energy-conversion efficiency, the excited electron and hole pairs should dissociate into separate positive and negative charges to escape from recombination due to the coulombic attraction. To achieve this process, the binding energy has to be overcome. That is, the dye molecule should posses less exciton binding energy for high energy conversion. Here, the exciton binding energy was calculated using the formula,[58, 59]

$$E_b = E_g - E_X = E_{H-L} - \lambda_{\max}$$

where, E_g is the band gap and is approximated as the HOMO-LUMO energy difference and E_X is the optical gap and is defined as the first singlet excitation energy, $\lambda_{\max}$. The calculated exciton binding energy of the designed molecules is summarized in Table 2. The exciton binding energy of QT1 molecule is 0.11 eV and that of the QT4, QT5 and QT6 molecules have nearly the same value. From Table 3, it has been observed that the exciton binding energy of QT2A and QT2B is same and is equal to 0.04 eV which is lesser than that of the other molecules. Note that the substitution of EWG on QT2B increases the exciton binding energy and the CF_3 substituted molecule has the maximum value of 0.34 eV. The above results show that the QT2, QT4, QT5 and QT6 molecules are more suitable for DSSC applications and substitution of EWG on the π-spacer will not provide high photo-current conversion efficiency.

3.4 Dipole Moment

The dipole moment is one of the important parameters which provide information about the electronic charge distribution in the molecule. The knowledge on the dipole moment of the organic molecule is important while designing the materials for opto-electronic applications. The calculated ground state dipole moment of the studied dye molecules in gas phase and in acetonitrile medium at B3LYP/6-311+G(2d,2p) level of theory is summarized in Table 3. The dipole moment of QT1 molecule in gas phase is 13.58 Debye. Except for QT3, QT4B and QT6

Physical Chemistry Chemical Physics Accepted Manuscript

molecules, the dipole moment of the designed molecules is higher than that of QT1. The EWG substituted derivatives possess higher dipole moment and notably the CF_3 substituted derivative has a dipole moment of 25.42 Debye in gas phase. From Table 3, it has been observed that the dipole moment of the quinoidal thiophene dye molecules have increased significantly in the acetonitrile medium. This is because of the additional dipole moment induced by the solvent reaction field. In acetonitrile medium, the dipole moment of QT1 molecule is 21.49 Debye and among the designed molecules, the NO_2 substituted dye molecule exhibit the maximum dipole moment of 55.68 Debye.

3.5 Static Polarizability and First Hyperpolarizability

The static polarizability (α) and first hyperpolarizability (β) of the quinoidal thiophene molecules were calculated using the formulas as described in previous study[29] and are summarized in Table 3. The static polarizability of QT1 is 571 a.u. The methoxy triphenylamine substituted QT molecule, QT5 has the maximum polarizability of 1364 a.u. The static polarizability is directly proportional to the dipole moment[60] and according to this proportionality the EWG substituted quinoidal thiophene molecules must have larger polarizability. But, from Table 3, it is found that the α value of Cl and Br substituted molecules is 1149 and 1088 a.u. whereas the α of other EWG substituted molecules is small due to the less contribution of α_{xx} component.

From Table 3, it has been found that the first hyperpolarizability of the studied molecules have increased with the increase in π-conjugation, except for QT2B molecule. The first hyperpolarizability is inversely proportional to the transition energy.[60] Accordingly, CF_3 substituted molecule with minimum transition energy (1.19 eV obtained from TDDFT calculation) exhibit the maximum β value of 74.64×10^{-28} esu. The strong electronegative fluorine

Physical Chemistry Chemical Physics Accepted Manuscript

atom in CF_3 provides the significant contribution of β_{yyy} component on β. That is, the displacement of charge cloud is higher in that particular direction. From Table 1, it is noted that the transition energy of the EWG substituted molecules is lesser than that of other molecules and consequently the β of these molecules is higher than that of other molecules. The above results are in line with the previous studies that the β depends on the donor, acceptor, π-bridge and functional group substitutions.[26, 27] Higher value of first hyperpolarizability and dipole moment is important for active NLO performance and the present results clearly inculcate that these quinoidal thiophene dye molecules particularly EWG substituted QT2B molecules can be used for NLO applications.

Physical Chemistry Chemical Physics Accepted Manuscript

4. Conclusions

By analyzing the results obtained using different DFT functionals and basis sets, it has been observed that B3LYP/6-311+G(2d,2p) level of theory predicts the experimental absorption wavelength for cyano-[5'-(4''-(N,N-dimethylamino)benzylidene)-5H-thiophen-2'-ylidene] acetic acid (QT1) molecule. The calculated absorption spectra of the designed quinoidal thiophene (QT) molecules indicate that the extension of π-conjugation through the quinoidal thiophene ring and the substitution of electron withdrawing groups on the QT rings increase the absorption wavelength significantly. The results obtained from the frontier molecular orbital analysis, free energy change for electron injection and exciton binding energy of the designed dye molecules show that the designed QT molecules with dimethyl-phenylamine, triphenylamine, methoxy substituted triphenylamine and naphthalene substituted groups as donors are more suitable for the DSSC application. Hence, it is expected that the results obtained from this investigation will have substantial impact on the development of DSSC based on quinoidal thiophene dye molecules. The calculated free energy change for electron injection on the dye molecules show that the relaxation effect is more in EWG substituted QT2B molecules, that is, the EWG substitution on QT2B molecule is not suitable for DSSC application. The calculated dipole moment, static polarizability and first hyperpolarizability values show that the EWG substituted QT2B molecules possess good NLO property.

Physical Chemistry Chemical Physics Accepted Manuscript

Supplementary Information The density plot of the orbitals involved in electronic transitions are shown in Figure S1.

Physical Chemistry Chemical Physics Accepted Manuscript

References

1 V. Tamilavan, A. Y. Kim, H. B. Kim, M. Kang and M. H. Hyun, *Tetrahedron*, 2014, **70**, 371-379.
2 L. L. Li and E. W. G. Diau, *Chem. Soc. Rev.*, 2013, **42**, 291-304.
3 A. Hagfeldt, G. Boschloo, L. Sun, L. Kloo and H. Pettersson, *Chem. Rev.*, 2010, **110**, 6595-6663.
4 J. Yang, P. Ganesan, J. l. Teuscher, T. Moehl, Y. J. Kim, C. Yi, P. Comte, K. Pei, T. W. Holcombe, M. K. Nazeeruddin, J. Hua, S. M. Zakeeruddin, H. Tian and M. Grätzel, *J Am. Chem. Soc.*, 2014, **136**, 5722-5730.
5 S. Urnikaite, T. Malinauskas, I. Bruder, R. Send, V. Gaidelis, R. d. Sens and V. Getautis, *J. Phys. Chem. C*, 2014, **118**, 7832-7843.
6 M. K. Nazeeruddin, P. Pechy, T. Renouard, S. M. Zakeeruddin, R. Humphry-Baker, P. Comte, P. Liska, L. Cevey, E. Costa, V. Shklover, L. Spiccia, G. B. Deacon, C. A. Bignozzi and M. Grätzel, *J. Am. Chem. Soc.*, 2001, **123**, 1613-1624.
7 M. K. Nazeeruddin, A. Kay, I. Rodicio, R. Humphry-Baker, E. Mueller, P. Liska, N. Vlachopoulos and M. Grätzel, *J. Am. Chem. Soc.*, 1993, **115**, 6382-6390.
8 M. K. Nazeeruddin, S. M. Zakeeruddin, R. Humphry-Baker, M. Jirousek, P. Liska, N. Vlachopoulos, V. Shklover, C. H. Fischer and M. Grätzel, *Inorg. Chem.*, 1999, **38**, 6298-6305.
9 M. K. Nazeeruddin, T. Bessho, L. Cevey, S. Ito, C. Klein, F. De Angelis, S. Fantacci, P. Comte, P. Liska, H. Imai and M. Grätzel, *J. Photochem. Photobiol. A*, 2007, **185**, 331-337.
10 P. Mathew, A. Yella, P. Gao, R. Humpery-Baker, B. F. E. Curchod, N. Ashari-Astanil, I. Tavernelli, U. Rothlisberger, M. K. Nazeeruddin and M. Gratzel, *Nat. Cem.*, 2014.
11 T. Bessho, S. M. Zakeeruddin, C. Y. Yeh, E. W. G. Diau and M. Grätzel, *Ang. Chem. Int. Ed.*, 2010, **49**, 6646-6649.
12 V. Venkatraman, P. O. Astrand and B. Kare Alsberg, *J. Comput. Chem.*, 2014, **35**, 214-226.
13 H. Li and M. Chen, *J. Mol. Model.*, 2013, **19**, 5317-5325.
14 R. Yeh-Yung Lin, H. W. Lin, Y. S. Yen, C. H. Chang, H. H. Chou, P. W. Chen, C. Y. Hsu, Y. C. Chen, J. T. Lin and K. C. Ho, *Energy Environ. Sci.*, 2013, **6**, 2477-2486.
15 J. Warnan, J. Gardner, L. Le Pleux, J. Petersson, Y. Pellegrin, E. Blart, L. Hammarstrom and F. Odobel, *J. Phys. Chem. C*, 2014, **118**, 103-113.
16 C.-Y. Tseng, F. Taufany, S. Nachimuthu, J.-C. Jiang and D.-J. Liaw, *Org. Electronics*, 2014, **15**, 1205-1214.
17 N. Santhanamoorthi, K.-H. Lai, F. Taufany and J.-C. Jiang, *J. Power Sources*, 2013, **242**, 464-471.
18 P. Liu, J.-j. Fu, M.-s. Guo, X. Zuo and Y. Liao, *Comput. Theor. Chem.*, 2013, **1015**, 8-14.
19 M. Komatsu, J. Nakazaki, S. Uchida, T. Kubo and H. Segawa, *Phys. Chem. Chem. Phys.*, 2013, **15**, 3227-3232.
20 C. Li, M. Liu, N. G. Pschirer, M. Baumgarten and K. Mullen, *Chem. Rev.*, 2010, **110**, 6817-6855.
21 H. Choi, C. Baik, S. O. Kang, J. Ko, M.-S. Kang, M. K. Nazeeruddin and M. Grätzel, *Angew. Chem.*, 2008, **120**, 333-336.

Physical Chemistry Chemical Physics Accepted Manuscript

22 K. Hara, T. Sato, R. Katoh, A. Furube, T. Yoshihara, M. Murai, M. Kurashige, S. Ito, A. Shinpo, S. Suga and H. Arakawa, *Adv. Funct. Mater.*, 2005, **15**, 246-252.

23 M. Yuan, M. M. Durban, P. D. Kazarinoff, D. F. Zeigler, A. H. Rice, Y. Segawa and C. K. Luscombe, *J. Polym. Sci. Part A: Polym. Chem*, 2013, **51**, 4061-4069.

24 R. Ma, P. Guo, L. Yang, L. Guo, X. Zhang, M. K. Nazeeruddin and M. Gratzel, *J. Phys. Chem. A.*, 2010, **114**, 1973-1979.

25 J. Feng, Y. Jiao, W. Ma, M. K. Nazeeruddin, M. Gratzel and S. Meng, *J. Phys. Chem. C*, 2013, **117**, 3772-3778.

26 Z. Benkova, I. Cernusak and P. Zahradnik, *Struct. Chem.*, 2006, **17**, 287-300.

27 M. C. R. Delgado, J. Casado, V. Hernandez, J. T. L. Navarrete, J. Orduna, B. Villacampa, R. Alicante, J. M. Raimundo, P. Blanchard and J. Roncali, *J. Phys. Chem. C* 2008, **112**, 3109-3120.

28 Y. Liu, G. Yang, S. Sun and Z. Su, *Chin. J. Chem.*, 2012, **30**, 2349-2355.

29 R. Nithya, M. Sowmiya, P. Kolandaivel and K. Senthilkumar, *Struct. Chem.*, 2014, **25**, 715-731.

30 A. D. Becke, *J. Chem. Phys.*, 1993, **98**, 5648-5652.

31 C. T. Lee, W. Yang and R. G. Parr, *Phys. Rev. B.*, 1988, **37**, 785-789.

32 S. H. Vosko, L. Wilk and M. Nusair, *Can. J. Phys.*, 1980, **58**, 1200-1211.

33 S. Miertus, E. Scrocco and J. Tomasi, *Chem. Phys.*, 1981, **55**, 117-129.

34 S. Manzhos, H. Segawa and K. Yamashita, *chem. Phys. Lett.*, 2012, **527**, 51-56.

35 M. Pastore, E. Mosconi, F. D. Angelis and M. Gratzel, *J. Phys. Chem. C*, 2010, **114**, 7205-7212.

36 P. Dev, S. Agrawal and N. J. English, *J. Chem. Phys.*, 2012, **136**, 224301.

37 J. P. Perdew, K. Burke and M. Ernzerhof, *Phys. Rev. Lett.*, 1996, **77**, 3865-3868.

38 J. P. Perdew, K. Burke and M. Ernzerhof, *Phys. Rev. Lett.*, 1997, **78**, 1396.

39 A. D. Becke, *J. Chem. Phys.* , 1993, **98**, 1372.

40 Y. Zhao and D. G. Truhlar, *Theor. Chem. Acc.*, 2008, **120**, 215-241.

41 Y. Zhao and D. G. Truhlar, *J. Phys. Chem. A.*, 2006, **110**, 13126-13130.

42 T. Yanai, D. P. Tew and N. C. Handy, *Chem. Phys. Lett.*, 2004, **393**, 51-57.

43 Y. Tawada, T. Tsuneda, S. Yanagisawa, T. Yanai and K. Hirao, *J. Chem. Phys.*, 2004, **120**, 8425.

44 H. Iikura, T. Tsuneda, T. Yanai and K. Hirao, *J. Chem. Phys.*, 2001, **115**, 3540.

45 A. S. Shalabi, A. M. El Mahdy, M. M. Assem, H. O. Taha and W. S. Abdel Halim, *Mol. Physics.*, 2014, **112**, 22-34.

46 J. Chen, J. Wang, F.-Q. Bai, Q.-J. Pan and H.-X. Zhang, *Int. J. Quant. Chem.*, 2013, **113**, 891-901.

47 W. Sang-aroon, S. Laopha, P. Chaiamornnugool, S. Tontapha, S. Sackow and V. Amornkitbamrung, *J. Mol. Model*, 2013, **19**, 1407-1415.

48 S. I. Gorelsky, *revision 5.0*, 2013, http://www.sg-chem.net/.

49 S. I. Gorelsky and A. B. P. Lever, *Organomet. Chem.*, 2001, **635**, 187-196.

50 J. B. Asbury, Y. Q. Wang, E. Hao, H. Ghosh and T. Lian, *Res. Chem. Interned.*, 2001, **27**, 393-406.

51 A. G. Al-Sehemi, A. Irfan, A. M. Asiri and Y. A. Ammar, *Spectrochim. Acta Part A: Molec. Biomolec. Spec.*, 2012, **91**, 239-243.

52 G. L. Gibson, T. M. McCormick and D. S. Seferos, *J. Am. Chem. Soc.*, 2012, **134**, 539-547.

Physical Chemistry Chemical Physics Accepted Manuscript

53 J. Preat, D. Jacquemin, C. Michaux and E. A. Perpete, *Chem. Phys.*, 2010, **376**, 56-68.
54 J. Preat, C. Michaux, D. Jacquemin and E. A. Perpete, *J. Phys. Chem. C*, 2009, **113**, 16821-16833.
55 J. Preat, *J. Phys. Chem. C*, 2010, **114**, 16716-16725.
56 A. Hagfeldt and M. Grätzel, *Chem. Rev.*, 1995, **95**, 49-68.
57 D. Vijay, E. Varathan and V. Subramanian, *J. Mater. Chem. A* 2013, **1**, 4358-4369.
58 G. D. Scoles and G. Rumbles, *Nat. Mater.*, 2006, **5**, 683.
59 Y. Li, T. Pullerits, M. Zhao and M. Sun, *J. Phys. Chem. C*, 2011, **115**, 21865-21873.
60 M. R. S. A. Janjua, M. U. Khan, B. Bashir, M. A. Iqbal, Y. Song, S. A. R. Naqvi and Z. A. Khan, *Comput. Theor. Chem.*, 2012, **994**, 34-40.

Physical Chemistry Chemical Physics Accepted Manuscript

Table 1 Absorption wavelength (λ_{abs} in nm and eV), oscillator strength (f in a.u.), orbital transitions and light harvesting efficiency (LHE) of the studied quinoidal thiophene dyes calculated at B3LYP/6-311+G(2d,2p) level of theory in acetonitrile medium.

Dyes	Electronic Transitions	λ_{abs}		f	LHE	Transition Assignment
		nm	eV			
QT1	$S_0 \rightarrow S_1$	539	2.30	1.382	0.959	H→L (+100%)
	$S_0 \rightarrow S_2$	373	3.33	0.031	0.069	H-1→L (+90%)
	$S_0 \rightarrow S_3$	327	3.79	0.016	0.036	H-2→L (+92%)
QT2A	$S_0 \rightarrow S_1$	661	1.87	1.952	0.989	H→L (+100%)
	$S_0 \rightarrow S_7$	329	3.77	0.020	0.045	H-3→L (+52%)
	$S_0 \rightarrow S_8$	324	3.82	0.067	0.143	H-5→L (+91%)
	$S_0 \rightarrow S_{10}$	308	4.02	0.070	0.149	H→L+2 (+59%) H→L+3 (30%)
QT2B	$S_0 \rightarrow S_1$	684	1.81	1.859	0.986	H→L (+100%)
	$S_0 \rightarrow S_2$	475	2.61	0.024	0.054	H-1→L (+86%)
	$S_0 \rightarrow S_3$	385	3.22	0.032	0.071	H→L+1 (+83%)
QT3	$S_0 \rightarrow S_1$	584	2.12	1.292	0.949	H→L (+100%)
	$S_0 \rightarrow S_2$	408	3.04	0.244	0.430	H-1→L (+95%)
	$S_0 \rightarrow S_5$	330	3.75	0.032	0.071	H→L+2 (+41%) H-3→L (+28%) H→L+1(25%)
	$S_0 \rightarrow S_6$	327	3.79	0.103	0.211	H-4→L (+56%) H-7→L (+31%)
QT4A	$S_0 \rightarrow S_1$	693	1.79	1.931	0.988	H→L (+99%)
	$S_0 \rightarrow S_2$	500	2.48	0.179	0.338	H-1→L (+93%)
	$S_0 \rightarrow S_6$	355	3.49	0.018	0.041	H-3→L (+43%) H-5→L (29%) H-2→L (22%)
QT4B	$S_0 \rightarrow S_1$	713	1.74	1.894	0.987	H→L (+99%)
	$S_0 \rightarrow S_2$	516	2.40	0.105	0.215	H-1→L (+93%)
	$S_0 \rightarrow S_3$	405	3.06	0.023	0.052	H→L+1 (+73%) H-2→L (+20%)
QT5	$S_0 \rightarrow S_1$	739	1.68	1.907	0.988	H→L (+100%)
	$S_0 \rightarrow S_2$	543	2.28	0.160	0.308	H-1→L (+95%)
	$S_0 \rightarrow S_3$	425	2.92	0.018	0.041	H-3→L (+54%) H→L+1 (+42%)
QT6	$S_0 \rightarrow S_1$	720	1.72	1.968	0.989	H→L (+99%)
	$S_0 \rightarrow S_2$	531	2.34	0.136	0.269	H-1→L (+95%)
	$S_0 \rightarrow S_4$	404	3.07	0.024	0.054	H→L+1 (+76%)
QT2B-Cl	$S_0 \rightarrow S_1$	760	1.63	1.358	0.957	H→L (+100%)
	$S_0 \rightarrow S_2$	499	2.48	0.432	0.630	H-1→L (+88%)
	$S_0 \rightarrow S_4$	405	3.06	0.038	0.083	H→L+1 (+80%)
QT2B-Br	$S_0 \rightarrow S_1$	828	1.50	0.847	0.856	H→L (+100%)
	$S_0 \rightarrow S_2$	505	2.46	0.639	0.770	H-1→L (+89%)
	$S_0 \rightarrow S_3$	462	2.68	0.015	0.034	H-2→L (+95%)
QT2B-CF_3	$S_0 \rightarrow S_1$	1043	1.19	0.085	0.178	H→L (+100%)
	$S_0 \rightarrow S_2$	451	2.75	1.140	0.928	H-1→L (+91%)
	$S_0 \rightarrow S_3$	401	3.09	0.038	0.084	H-2→L (+83%)
QT2B-CN	$S_0 \rightarrow S_1$	861	1.44	0.625	0.763	H→L (+100%)
	$S_0 \rightarrow S_2$	528	2.35	0.534	0.708	H→L+1(+81%) H-1→L (18%)
	$S_0 \rightarrow S_3$	469	2.64	0.373	0.576	H-1→L (+77%) H→L+1 (+18%)
QT2B-NO_2	$S_0 \rightarrow S_1$	880	1.41	0.243	0.429	H→L (+100%)
	$S_0 \rightarrow S_2$	651	1.90	0.089	0.185	H→L+1 (+97%)
	$S_0 \rightarrow S_4$	536	2.31	0.012	0.027	H→L+2 (+66%) H→L+3(+29%)

Physical Chemistry Chemical Physics Accepted Manuscript

Table 2 The calculated redox potential of the ground state (E_{OX}^{dye} in eV), oxidation potential of the dye ($E_{OX}^{dye^*}$ in eV), absorption energy (λ in eV), free energy change for electron injection (ΔG_{inject} in eV), energy gap ($E_{H\text{-}L}$ in eV) and exciton binding energy (E_b in eV) of the studied dye molecules at B3LYP/6-311+G(2d,2p) level of theory in acetonitrile medium.

Dyes	**Unrelaxed**				**Relaxed**			**$E_{H\text{-}L}$**	**E_b**
	E_{OX}^{dye}	λ	$E_{OX}^{dye^*}$	ΔG_{inject}	E_{0-0}^{dye}	$E_{OX}^{dye^*}$	ΔG_{inject}		
QT1	5.50	2.3	3.20	-0.80	2.25	3.25	-0.75	2.41	0.11
QT2A	5.22	1.87	3.35	-0.65	1.81	3.41	-0.59	1.91	0.04
QT2B	5.22	1.81	3.41	-0.59	1.74	3.48	-0.52	1.85	0.04
QT3	5.53	2.12	3.41	-0.59	1.89	3.64	-0.36	2.33	0.21
QT4A	5.29	1.79	3.50	-0.50	1.71	3.58	-0.42	1.9	0.11
QT4B	5.27	1.74	3.53	-0.47	1.66	3.61	-0.39	1.84	0.10
QT5	5.17	1.68	3.49	-0.51	1.60	3.57	-0.43	1.78	0.10
QT6	5.27	1.72	3.55	-0.45	1.64	3.63	-0.37	1.84	0.12
QT2B-Cl	5.45	1.63	3.82	-0.18	1.17	4.28	0.28	1.7	0.07
QT2B-Br	5.46	1.5	3.96	-0.04	1.10	4.36	0.36	1.64	0.14
QT2B-CF_3	5.62	1.19	4.43	0.43	0.92	4.70	0.70	1.53	0.34
QT2B-CN	5.82	1.44	4.38	0.38	1.06	4.76	0.76	1.64	0.20
QT2B-NO_2	5.95	1.41	4.54	0.54	1.07	4.88	0.88	1.7	0.29

Physical Chemistry Chemical Physics Accepted Manuscript

Table 3 The dipole moment (in Debye), polarizability α (in a.u.) and first hyperpolarizability β (in $x10^{-28}$ esu) of the studied quinoidal thiophene dyes calculated at B3LYP/6-311+G(2d,2p) level of theory in acetonitrile medium.

Dyes	Dipole Moment		α	β
	Gas phase	Acetonitrile		
QT1	13.58	21.49	571	2.33
QT2-A	17.29	30.02	1008	2.56
QT2-B	17.76	32.26	1034	1.82
QT3	11.68	17.67	768	5.40
QT4-A	14.85	24.70	1214	10.51
QT4-B	12.80	23.67	1245	10.88
QT5	16.50	28.99	1364	13.52
QT6	12.86	23.45	1357	12.65
QT2B-Cl	19.62	43.40	1149	14.73
QT2B-Br	19.71	47.83	1088	23.22
QT2B-CF_3	25.42	50.34	684	74.64
QT2B-CN	24.08	51.36	992	19.25
QT2B-NO_2	24.28	55.68	796	12.25

Physical Chemistry Chemical Physics Accepted Manuscript

Figure Captions:

Figure 1. The chemical structures of the studied quinoidal thiophene dyes.

Figure 2. The energies of HOMO, LUMO and HOMO-LUMO gap in (eV) of quinoidal thiophene dyes calculated at B3LYP/6-311+G(2d,2p) level of theory in acetonitrile medium.

Figure 3. The ground state density plot of the highest occupied molecular orbital (HOMO) of quinoidal thiophene dyes calculated at B3LYP/6-311G(d,p) level of theory in acetonitrile medium.

Figure 4. The ground state density plot of the lowest unoccupied molecular orbital (LUMO) of quinoidal thiophene dyes calculated at B3LYP/6-311G(d,p) level of theory in acetonitrile medium.

Figure 5. The absorption spectra of the quinoidal thiophene dyes computed at TD-B3LYP/6-311+G(2d,2p) level of theory in acetonitrile medium.

Physical Chemistry Chemical Physics Accepted Manuscript

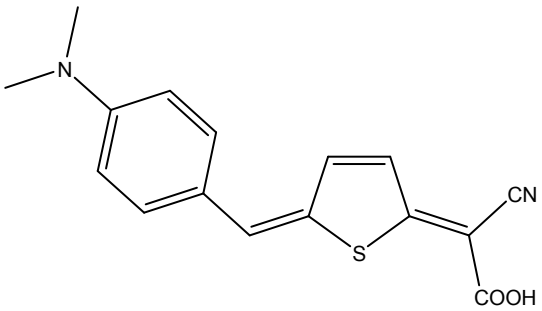

QT1

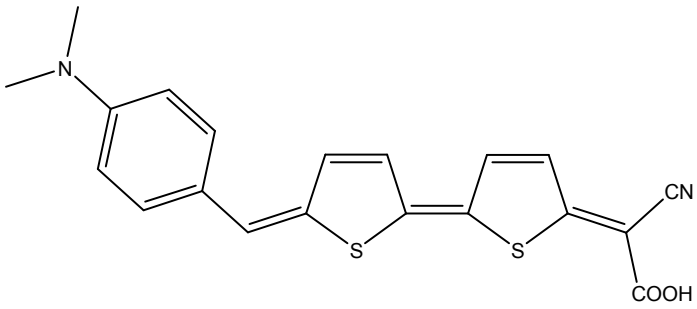

QT2A

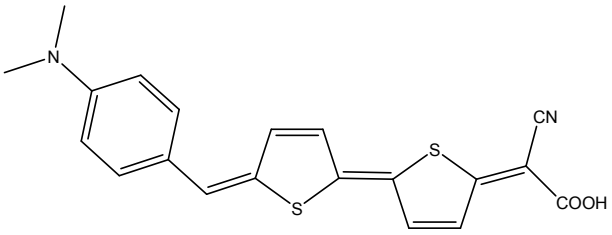

QT2B

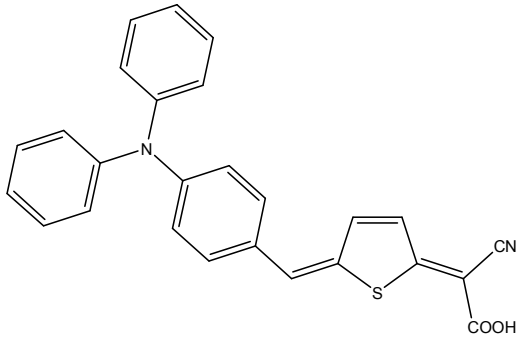

QT3

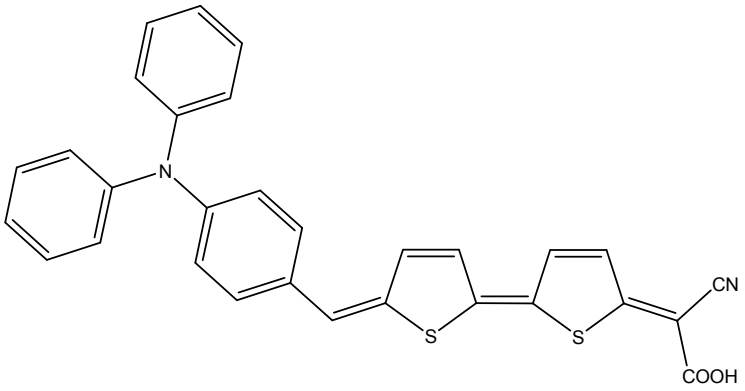

QT4A

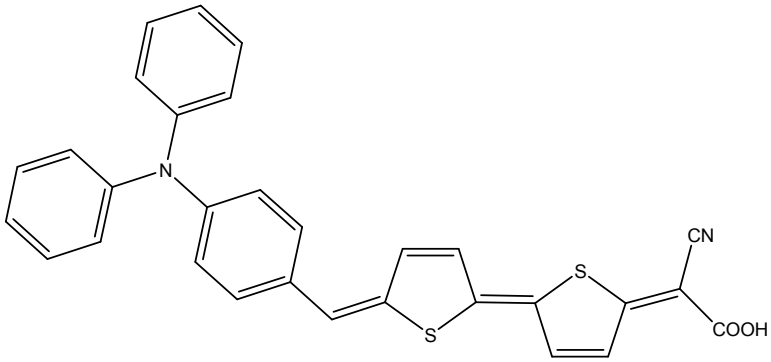

QT4B

Physical Chemistry Chemical Physics Accepted Manuscript

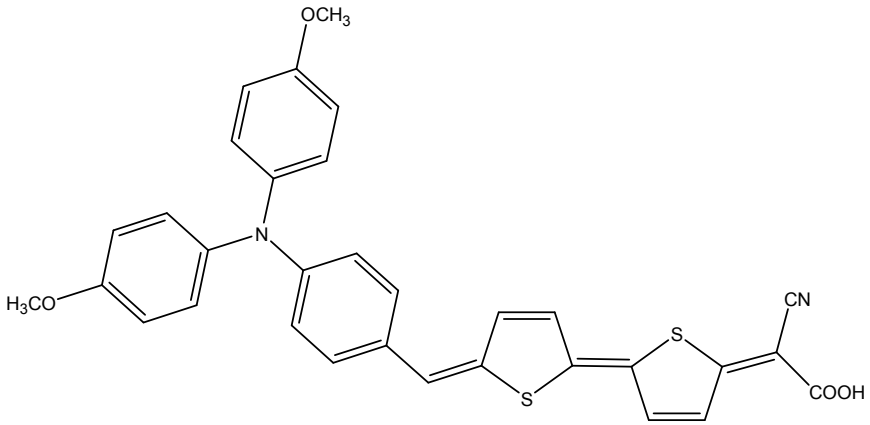

QT5

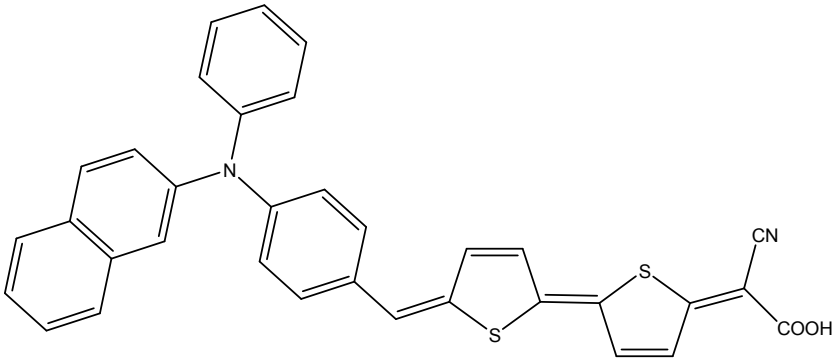

QT6

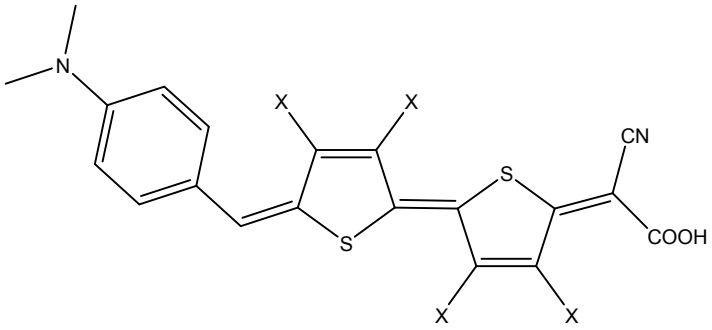

QT2B-X

X=Cl, Br, CF_3, CN and NO_2

Figure 1

Physical Chemistry Chemical Physics Accepted Manuscript

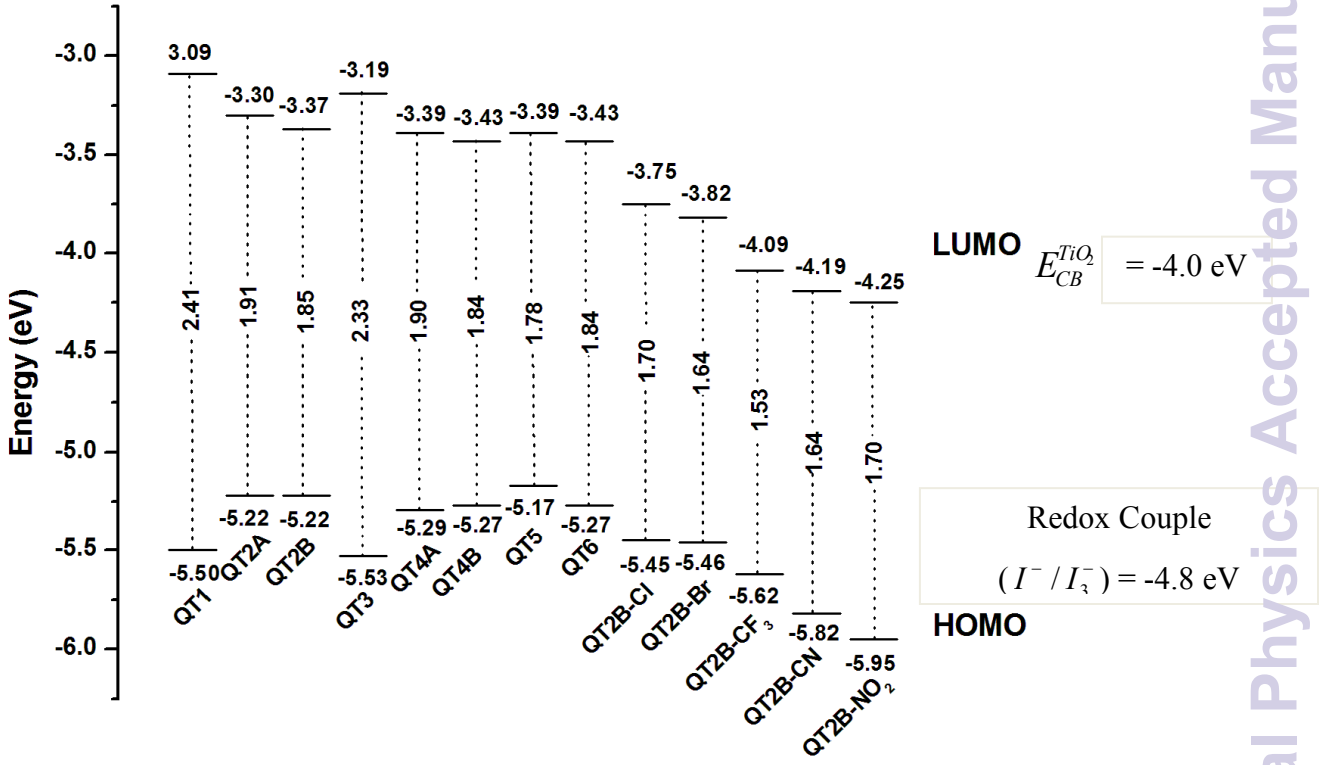

Figure 2

Physical Chemistry Chemical Physics Accepted Manuscript

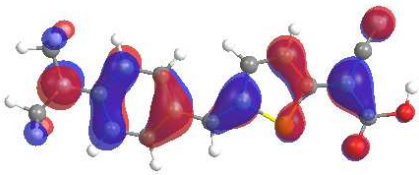

QT1

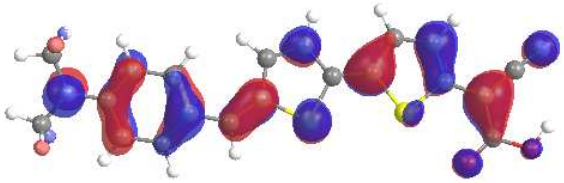

QT2A

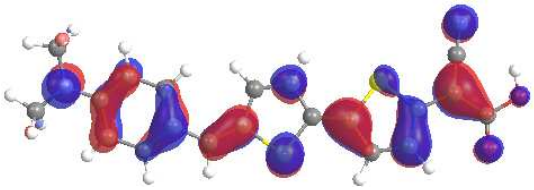

QT2B

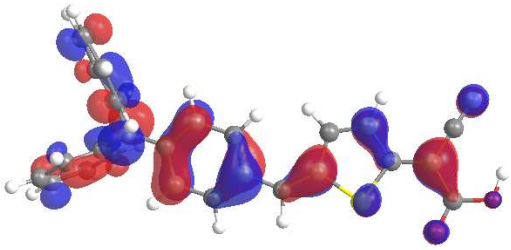

QT3

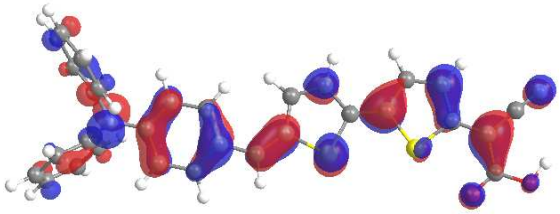

QT4A

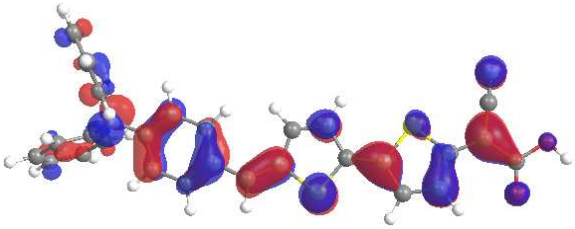

QT4B

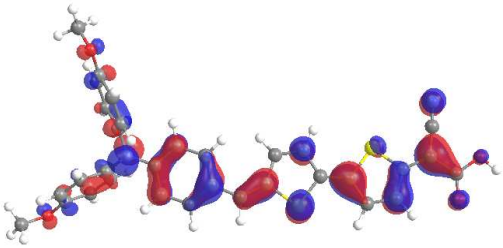

QT5

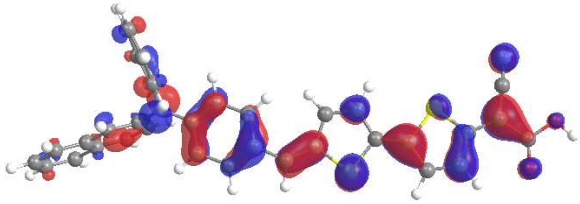

QT6

Physical Chemistry Chemical Physics Accepted Manuscript

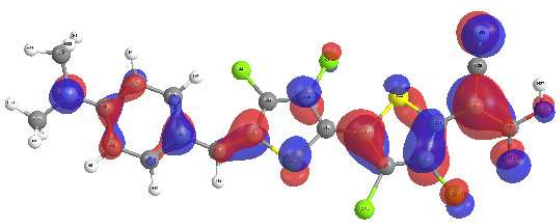

QT2B-Cl

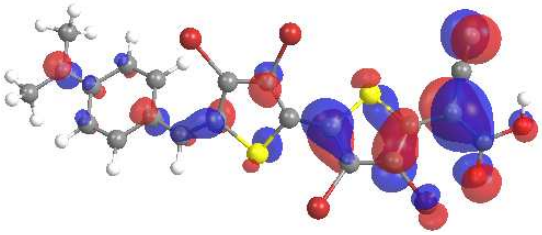

QT2B-Br

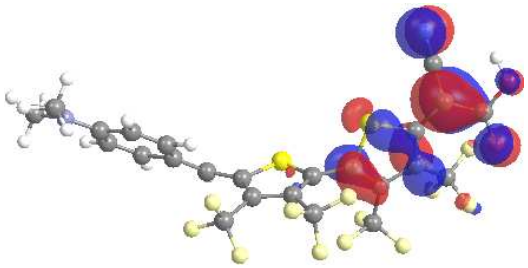

QT2B-CF_3

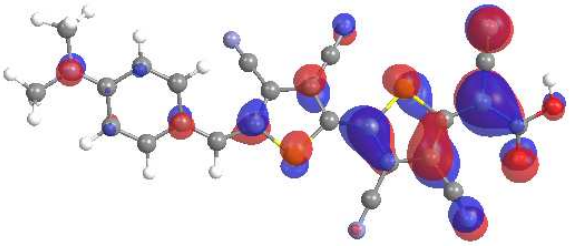

QT2B-CN

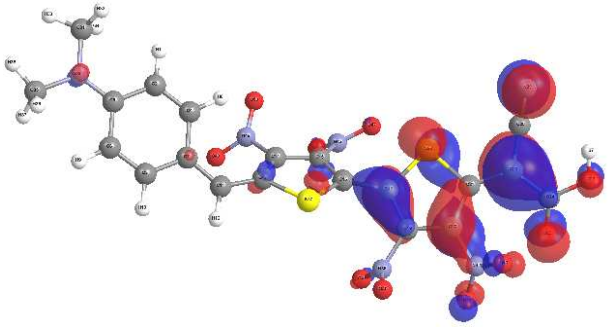

QT2B-NO_2

Figure 3

Physical Chemistry Chemical Physics Accepted Manuscript

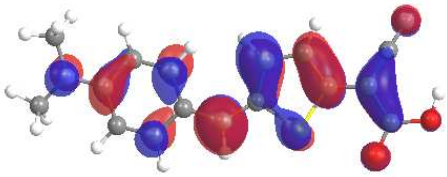

QT1

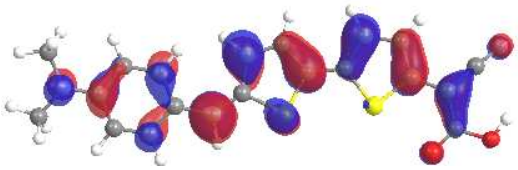

QT2A

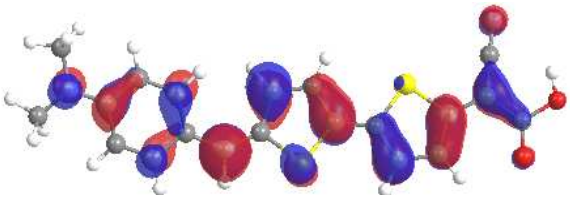

QT2B

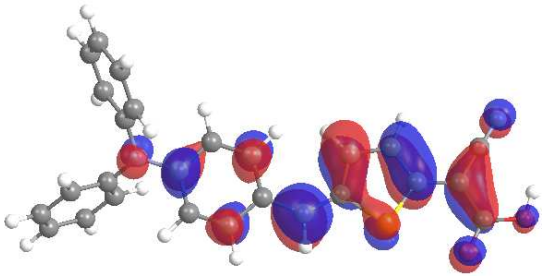

QT3

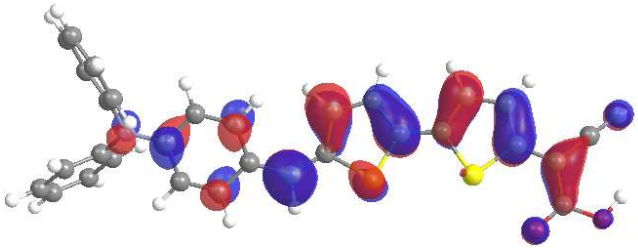

QT4A

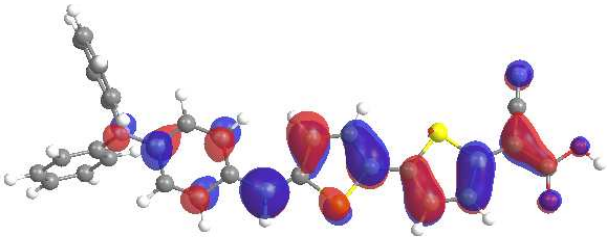

QT4B

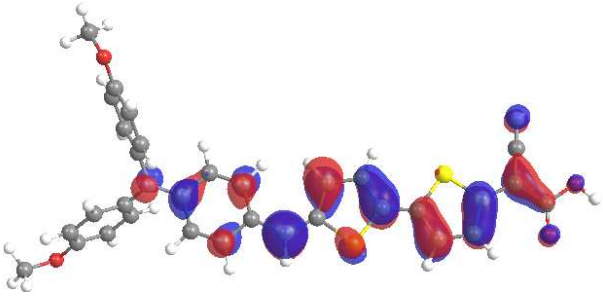

QT5

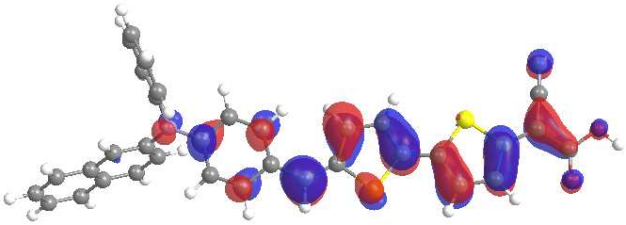

QT6

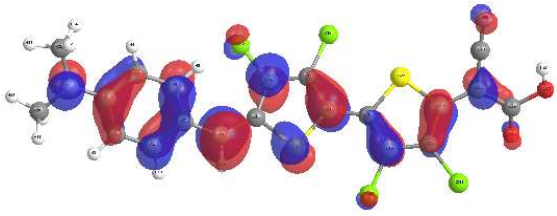

QT2B-Cl

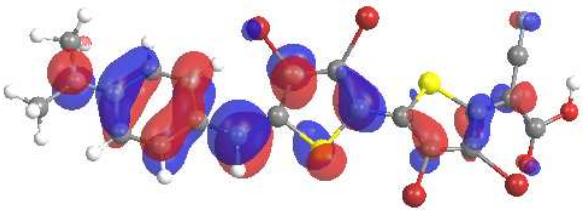

QT2B-Br

Physical Chemistry Chemical Physics Accepted Manuscript

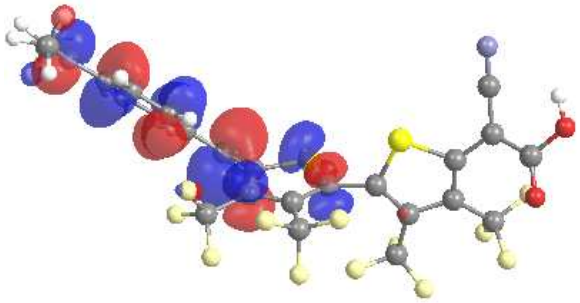

QT2B-CF_3

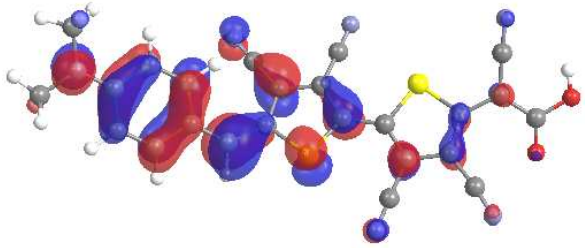

QT2B-CN

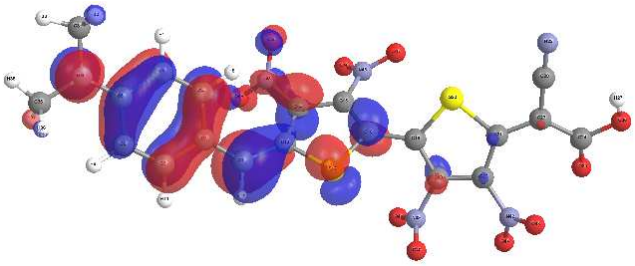

QT2B-NO_2

Figure 4

Physical Chemistry Chemical Physics Accepted Manuscript

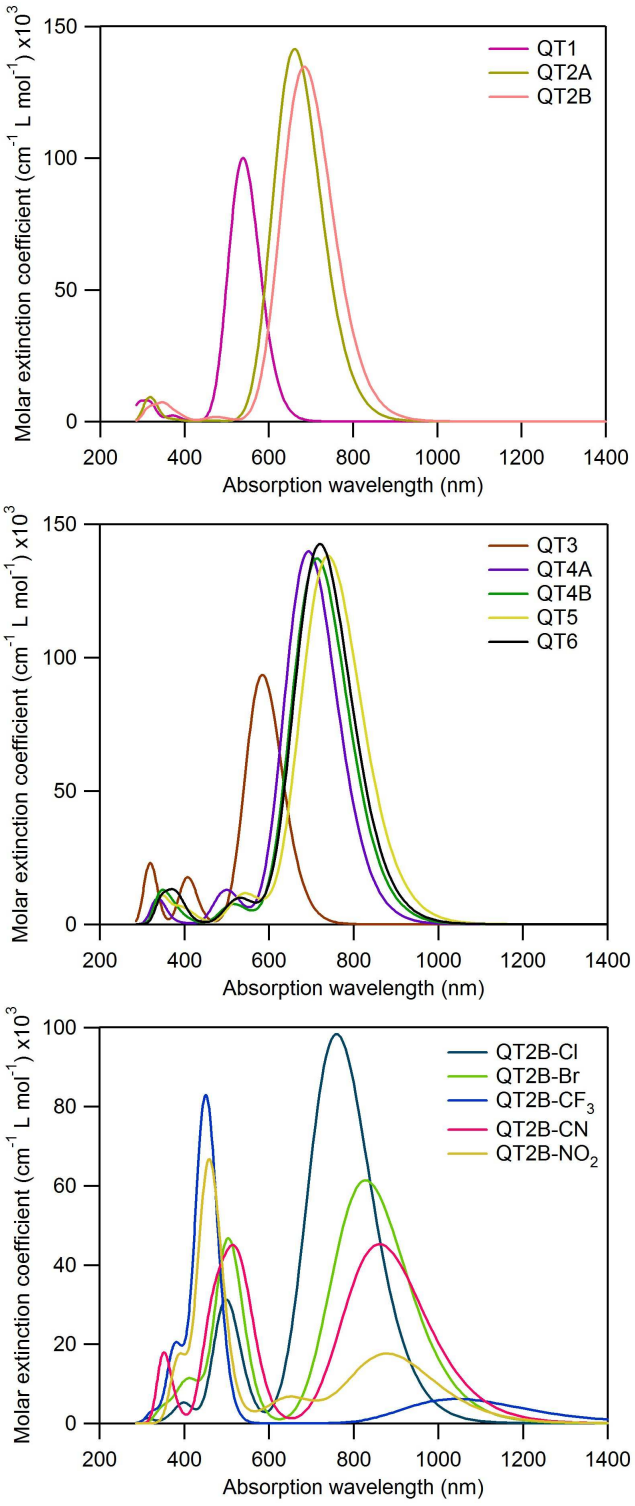

Figure 5

Physical Chemistry Chemical Physics Accepted Manuscript